Available online at www.sciencedirect.com
SCIENCE DIRECT
Earth and Planetary Science Letters 236 (2005) 856–870
EPSL
www.elsevier.com/locate/epsl

Room-temperature magnetic properties of ferrihydrite: A potential magnetic remanence carrier?

S. Johari Pannalal[a], Sean A. Crowe[a,b], Maria T. Cioppa[a], David T.A. Symons[a], Arne Sturm[a,b], David A. Fowle[a,b,*]

[a]*Department of Earth Sciences, University of Windsor, Windsor, ON N9B 3P4, Canada*
[b]*The Great Lakes Institute for Environmental Research (GLIER), University of Windsor, Windsor, ON N9B 3P4, Canada*

Received 24 May 2004; received in revised form 17 March 2005; accepted 18 May 2005
Available online 14 July 2005
Editor: E. Boyle

Abstract

Room-temperature magnetic techniques are rapidly becoming an important tool for the discrimination and quantification of minerals in a broad range of geological, environmental and extraterrestrial materials. The utility of these techniques is dependent upon the comprehensiveness and consistency of data describing the magnetic characteristics of individual mineral phases. In this regard, there is a paucity of data pertaining to the magnetic properties of ferrihydrite. This paper reports room-temperature magnetic properties of ferrihydrite that are relevant to studies concerning geological and environmental materials under surficial conditions. Synthetic ferrihydrite, both 2- and 6-line varieties, exhibit a susceptibility of ~2.7×10^{-6} m^3 kg^{-1} at 298 K. Significantly, at 298 K synthetic ferrihydrite exhibits a saturation remanent magnetization (σ_{RS}) of 1.19 and 0.86×10^{-4} A m^2 kg^{-1} for 2- and 6-line ferrihydrite, respectively. These observations suggest that ferrihydrite is a potential magnetic remanence carrier under ambient environmental conditions. Measurements of mineral mixtures show that magnetic techniques can discriminate between ferrihydrite and goethite at low concentrations. Natural samples of ferrihydrite exhibit magnetic properties that are consistent with those obtained for synthetic ferrihydrite. Thus, magnetic techniques using room-temperature magnetic properties may find important applications in studies of the biogeochemical cycling of Fe in dynamic settings.

Keywords: ferrihydrite; room-temperature; magnetic properties; susceptibility; environmental magnetism

1. Introduction

Ferrihydrite is a poorly crystalline Fe hydroxide and there is currently extensive debate over the exact nature and degree of ordering within its structure [1–5]. As a result, the term hydrous ferric oxide (HFO) is

* Corresponding author. Department of Earth Sciences, University of Windsor, Windsor, ON N9B 3P4, Canada. Tel.: +1 519 2533000x3763; fax: +1 519 9713616.
E-mail addresses: pannala@uwindsor.ca (S. Johari Pannalal), fowle@uwindsor.ca (D.A. Fowle).

0012-821X/$ - see front matter © 2005 Elsevier B.V. All rights reserved.
doi:10.1016/j.epsl.2005.05.019

often applied to describe these poorly crystalline Fe phases in order to distinguish them from minerals, sensu stricto, which possess long range internal order. In this paper the term "ferrihydrite" is used to describe such phases, however no assumptions are implied with respect to the exact nature of the internal ordering.

Ferrihydrite is widespread and occurs in a diverse suite of geological settings that range from aquatic sediments [6–8] to meteorites [9] and possibly even to Martian soils [10,11]. As ferrihydrite has a very high surface area to volume ratio, it is highly reactive. Thus, it is important in the biogeochemical cycling of iron and often controls the cycling of trace metals and nutrients such as phosphorus and organic matter [12–14]. In addition, ferrihydrite is important as a bioavailable source of Fe (III) for use as a terminal electron acceptor during anaerobic microbial metabolism [15,16]. In aquatic environments the precipitation of ferrihydrite commonly results from rapid changes in pH, temperature and/or redox potential, which frequently involves the participation of Fe oxidizing bacteria (e.g. *Gallionella* and *Leptothrix* sp.) [17,18]. Thus, it is common to find ferrihydrite in environments where mixing of water from different sources occurs, as for example, near mineral springs and supergene environments [19], downstream from acid-mine tailings [20], and proximal to deep-sea hydrothermal vents [21]. In fact, ferrihydrite produced near hydrothermal vents may have been critical for the development of early microbial life on Earth [22]. In terrestrial environments ferrihydrite is commonly produced as an intermediate weathering product of primary Fe oxides and sulphides that later recrystallizes to more stable phases such as goethite or hematite. Ferrihydrite can form a significant fraction of soils that are produced by rapid weathering such as tropical laterites, spodosols and podozols, which precludes the formation of the more stable iron (hydr)oxide phases [23]. The presence of abundant organic matter, trace metals, P, Si, and/or Al tend to retard crystal growth and can result in the long-term persistence of ferrihydrite in wet cool environments [23,24].

The degree of ferrihydrite crystallinity is variable and ranges from amorphous to poorly crystalline (2-line) ferrihydrite to an ordered (6-line) ferrihydrite. The 2- and 6-line varieties are characterized by XRD spectra with two broad peaks at 0.26 and 0.15 nm, and six broad peaks at 0.26, 0.221, 0.196, 0.172, 0.15 and 0.148 nm, respectively [25]. Due to the range of crystallinities, the stoichiometric composition of ferrihydrite is poorly defined. The simple formula $Fe(OH)_3$ is commonly used, however, more complex stoichiometries (e.g. Fe_2O_3•2FeOOH•26H_2O) have also been proposed [26]. The generally accepted structural model suggests octahedral coordinated Fe with a hexagonal unit cell similar to that of hematite [24]. Recent spectroscopic (EXAFS, XAFS and XANES) studies have provided evidence for both purely octahedral coordinated Fe [27–29] and mixed octahedral/tetrahedral coordination [30,31]. Interestingly, based on these spectroscopic studies, it has been proposed by Jambor and Dutrizac [24] that the cores of ferrihydrite comprise octahedral coordinated Fe whereas surfaces comprise both octahedral and tetrahedral coordinated Fe. Given the high surface area to volume ratio of ferrihydrite, these putative surface tetrahedral sites would have a significant influence on its physical and chemical properties.

The abundance, and therefore the importance, of ferrihydrite in modern geological environments has often been underestimated because of a lack of detection and recognition when present [24]. In natural samples, the combination of extremely fine grain size and poor crystallinity make ferrihydrite difficult to identify and quantify by conventional techniques such as powder XRD and SEM. Proxies, based on operationally defined chemical extractions (e.g. ammonium oxalate, [32]) are often used to estimate the quantity of easily extractable ferric iron. However, these extractions are fraught with complications. Perhaps the most serious of these is the partial dissolution of ferrous Fe phases (e.g. siderite), which results in an inaccurate estimate of ferrihydrite abundance. A recent extensive review by Jambor and Dutrizac [24] stressed the need for a reliable characterization procedure. The utility of mineral/rock magnetic properties to discriminate and quantify small amounts of iron oxides, sulphides and oxyhydroxides in natural samples is becoming increasingly recognized [33,34]. Such studies typically use various magnetic measurements to delineate the mineralogy, domain state, and concentration of ferri- or antiferromagnetic (i.e. minerals able to carry a remanent magnetization under ambient conditions) minerals in bulk samples [35]. Recently, Frederichs et al. [36] have also used

low-temperature magnetic properties to characterize paramagnetic minerals (siderite, rhodochrosite, and vivianite) in marine sediments.

Unfortunately, in comparison with other naturally occurring Fe phases there is relatively little literature pertaining to the magnetic properties of ferrihydrite. Furthermore, the existing literature is contradictory. Initial studies of ferrihydrite using Mössbauer spectroscopy suggested a superparamagnetic behaviour at room temperature (298 K) with an increase in magnetic ordering occurring at lower temperatures [37–40]. Pankhurst and Pollard [40] reported that synthetic ferrihydrites at 4.2 K are ferromagnetic for the 2-line variety and antiferromagnetic for the 6-line variety. Low-temperature (4–293 K) rock-magnetic (low-field susceptibility, isothermal remanent magnetization (IRM), coercive force, and high-field susceptibility) studies [41] of synthetic 6-line ferrihydrite suggest that the more crystalline variety is antiferromagnetic with a parasitic ferromagnetic component and a Néel temperature of 120 K. In addition, Zergenyi et al. [41] reported a room-temperature mass specific susceptibility (χ) value of $1.00 \pm 0.01 \times 10^{-6}$ m^3 kg^{-1} for the 6-line ferrihydrite.

In these preliminary studies, the room-temperature magnetic properties have been overlooked as potential identifiers of ferrihydrite. Rock magnetic and paleomagnetic studies that purport to examine environmental change and/or the effects of varying environmental conditions on magnetic signals are only useful when the conditions (geological, chemical, biochemical) governing or controlling the mineral magnetic properties have been identified and described. The presence of ferrihydrite in the diverse conditions described above suggests that it would be wise to characterize its magnetic properties under near surface conditions. Furthermore, the increasing use of paleomagnetic techniques (i.e. techniques using the natural remanence directions) in environmental and paleoclimatic studies using surficial sediments demands an understanding of the potential of ferrihydrite to carry magnetic remanence. To this end, measurements were made at room temperature of synthetic ferrihydrite, both 2- and 6-line varieties, to characterize their rock magnetic properties. In addition, mechanical mixtures of goethite and ferrihydrite have been used to test the utility of room-temperature magnetic properties for discriminating between these two minerals in mixed samples. In this work, rock magnetic properties have been used to identify and characterize ferrihydrite in marine sediments and aquifers.

2. Experimental

2.1. Synthesis and aging of synthetic iron oxyhydroxides

Synthesis of 2-line ferrihydrite was accomplished by titrating aqueous solutions of $FeNO_3$ [25] and $FeCl_3$ [42] up to pH 7.5. The resulting precipitate was centrifuged at 4000 $\times g$ and washed 5 times with 18 MΩ RO water (Barnstead nanopure). 6-line ferrihydrite was synthesized by adding 0.1 mol of $FeNO_3$•9 H_2O to 2 L of 18 MΩ RO water that was preheated to 75 °C. The $FeNO_3$ solution was maintained at 75 °C for an additional 20 min and then quenched to 5 °C in an ice bath. After warming to 25 °C the $FeNO_3$ solution was titrated with 1.0 M NaOH to a pH of 7.5. The resulting flocculent was centrifuged at 4000 $\times g$ and washed 5 times with 18 MΩ RO water. Magnetometry was performed directly on these flocculants as described below (Section 2.2). Synthetic goethite was prepared from aqueous $FeNO_3$ solutions after Cornell and Schwertmann [25]. Goethite and both 2- and 6-line ferrihydrites were freeze-dried at −50 °C and 100 mbar (ThermoSavant ModulyoD). The identity of these synthetic Fe oxyhydroxides was confirmed by powder XRD (Fig. 1). XRD analysis was performed using a Rigaku MiniFlex with Cu Kα radiation, a sampling interval of 0.05° and a scan rate of 1.00° min^{-1}. Background $K\alpha_2$ radiation was subtracted by fitting a cubic spline using MDI JADE XRD pattern processing software. Transmission Electron Microscopy (TEM) and High Resolution Transmission Electron Microscopy (HRTEM) (JEOL 2010F) revealed a poorly crystalline aggregate of equidimensional particles with grain sizes of approximately 3–5 nm (Fig. 1d). Electron microscopy failed to reveal the presence of highly crystalline minerals such as hematite and/or maghemite. These results are consistent with those of others using the similar synthesis protocols [e.g. 43,44]. Measurements of specific surface area (5-point, N_2-BET) yielded values of 2.29×10^2 m^2 g^{-1} and 2.527×10^2 m^2 g^{-1} for 2- and 6-line ferrihydrite

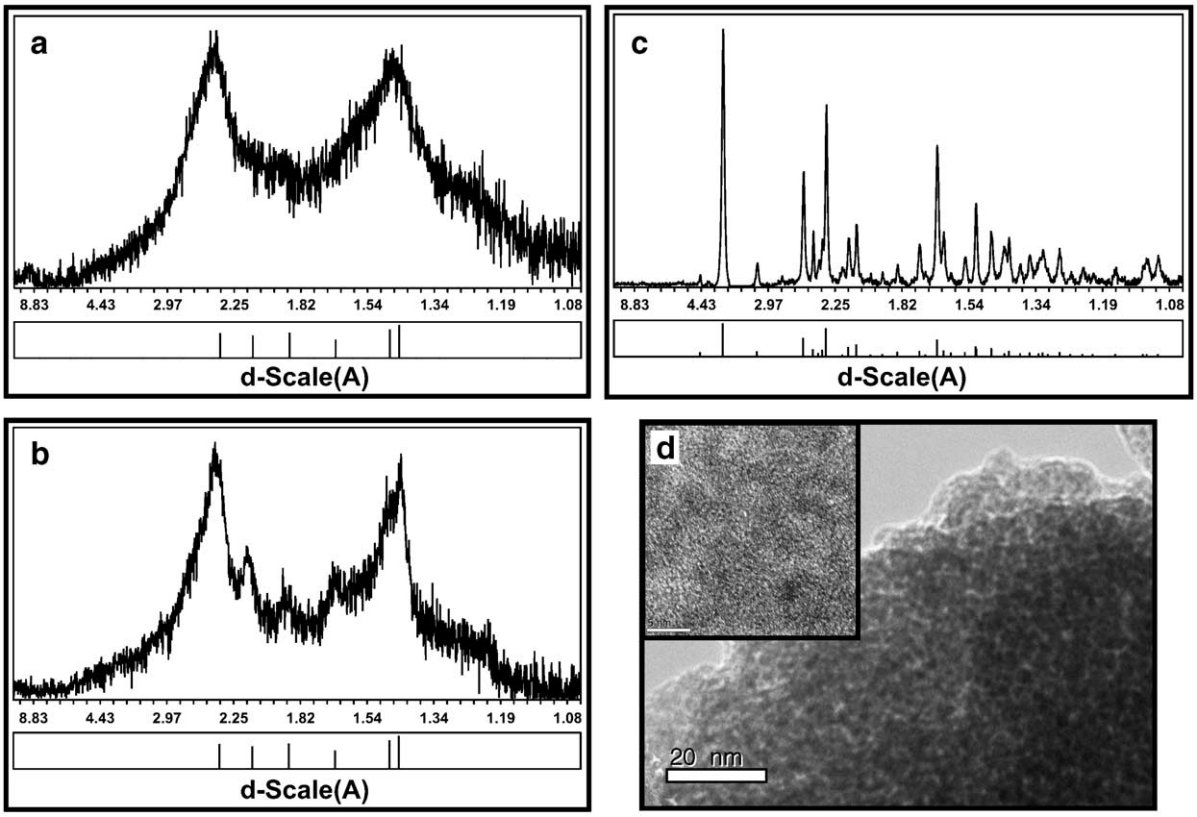

Fig. 1. Powder XRD patterns (a) synthetic 2-line ferrihydrite, (b) synthetic 6-line ferrihydrite, (c) synthetic goethite, and (d) TEM image of ferrihydrite showing aggregates of 3–5 nm spherical particles; inset is a high resolution image of poorly ordered 6-line ferrihydrite. Scale-bars are 20 and 5 nm in the main image and inset respectively.

respectively. These values are the same as those characteristic for 3–6 nm grains of ferrihydrite [25,26]. In order to assess the mineralogical stability of the ferrihydrite precipitates, samples were aged for 3 weeks in 0.25 M $NaNO_3$, 0.25 M NaCl, and 18 MΩ RO water. No detectable change in magnetic properties or diffraction patterns was observed over the 3 week period.

2.2. Rock/mineral magnetic measurements

All mineral magnetic measurements were performed in the Rock Magnetic and Paleomagnetic Laboratory in the Department of Earth Sciences, University of Windsor. Bulk magnetic susceptibility measurements were conducted using an AGICO Systems KLY-CS3 Kappa bridge. Changes in susceptibility with temperature were determined using the KLY-CS3 Kappa Bridge by cooling the sample to 77 K, using liquid nitrogen, followed by stepwise heating (1.5° min^{-1}) to 273 K. In addition, hysteresis loops with a maximum field of 1 T were measured on a Magnetic Measurements Variable Field Translation Balance (VFTB) at room temperature. Other mineral magnetic techniques including pulse magnetization, demagnetization and subsequent remanence measurements were conducted in a magnetically shielded room with an ambient field of <0.1% of the Earth's magnetic field. These measurements were conducted with repeats, to estimate precision, on both wet and freeze-dried 2- and 6-line ferrihydrite samples. A thin-walled plastic cylindrical sample holder, with a magnetic susceptibility of -3.7×10^{-6} SI, was used. The empty sample holders were demagnetized at 120 mT, using a Sapphire Instruments SI-4 demagnetizer, prior to any magnetic measurements. All of the remanence measurements were conducted using a 2 G Enterprises

755R DC-SQUID three-axis cryogenic magnetometer with an automated vertical sample handling system and a sensitivity of ~4.0×10^{-6} A/m. Prior to any magnetization or demagnetization procedures, all the samples were measured for the presence of natural remanent magnetization (NRM). The samples were alternating field (AF) demagnetized at 120 mT to remove the NRM component.

In order to determine the magnetic remanence characteristics, the samples were subjected to a series of magnetization and demagnetization protocols. To impart a magnetization, a 1.2 T direct field was applied to the samples using a Sapphire Instruments SI-6 pulse magnetizer. This induced remanence was then removed by AF demagnetization in 15 steps to 140 mT, with the remanence intensity measured after each step. Saturation remanence tests on the samples were conducted by applying a direct field in 16 steps to 1.2 T. The samples were subsequently AF demagnetized in 15 steps to 140 mT. Remanence measurements were conducted after each step during both magnetization and demagnetization protocols. All the magnetic measurements were performed on both wet and freeze-dried synthetic samples of 2- and 6-line ferrihydrite. The measurements on the wet samples were conducted within ~12 h of preparation.

2.3. Mixtures of goethite and ferrihydrite

Samples containing various quantities, based on mass, of synthetic goethite and ferrihydrite were prepared using a Denver Instrument APX 200 Analytical Balance. These samples were used to test the magnetic behaviours of environmentally relevant iron oxide mixtures. Samples were subjected to the same series of magnetic protocols as described in Section 2.2.

2.4. Preparation and measurement of natural samples

Two samples of sediment (SP1 and SP2) from the Äspö Hard Rock Laboratory (HRL) in southern Sweden [45], and one sediment sample (JDF) collected proximal to an axial volcano on the Juan de Fuca mid-ocean ridge [17], were obtained from Dr. C. Kennedy (University of Götenberg). The HRL samples were received wet and were refrigerated at 4 °C until analysis. The sample from the Juan de Fuca ridge was freeze-dried prior to receipt. Magnetic measurements were conducted, as described above, on both wet and freeze-dried samples from the seep, and on the freeze-dried sample from the Juan de Fuca ridge.

3. Results

3.1. Synthetic 2- and 6-line ferrihydrite

Magnetic susceptibilities for the synthetic ferrihydrite samples are presented in Table 1. Mass specific susceptibilities (χ) were calculated from the measured volume specific susceptibilities (κ_{SI}) after Peters and Dekkers [35]. Calculations of χ were made by dividing κ_{SI} by the known ferrihydrite density of 3.96 g cm^{-3} [37].

Two-line ferrihydrite (2-line) has κ_{SI} values that range from $5.577 \pm 0.006 \times 10^{-3}$ SI (1σ) (wet) to $10.08 \pm 0.01 \times 10^{-3}$ SI (1σ) (freeze-dried) when synthesized from chloride and nitrate solutions, respectively, which are equivalent to χ values of 1.468 ± 0.002 and $2.652 \pm 0.003 \times 10^{-6}$ m^3 kg^{-1} (1σ). Similarly 6-line ferrihydrite exhibits a κ_{SI} of $7.242 \pm 0.008 \times 10^{-3}$ SI (1σ) (wet) and $10.24 \pm 0.001 \times 10^{-3}$ SI (1σ) (freeze-dried), which correspond to χ values of 1.906 ± 0.002 and $2.69 \pm 0.003 \times 10^{-6}$ m^3 kg^{-1} (1σ). In addition, synthetic goethite gives a χ value, calculated from κ_{SI} as described above ($\rho = 4.26$ g cm^{-3}, [46]), of $1.357 \pm 0.001 \times 10^{-6}$ m^3 kg^{-1} (1σ) (Table 1). The AF decay of isothermal remanent magnetization, induced by a 1200 mT direct field, for all of the synthetic ferrihydrite samples shows a uniform and rapid decay (data not shown). Cross-over plots [47] showing the acquisition of saturation isothermal remanent magnetization (SIRM) and its decay on AF demagnetization are depicted in Fig. 2. These plots show a uniform acquisition of magnetization and saturation at ~200 mT for both 2- and 6-line mineral phases. The AF demagnetization of SIRM up to 140 mT shows a smooth decay with cross-overs of 30 and 40 mT for wet and freeze-dried ferrihydrite, respectively. Saturation remanent magnetization (M_{RS}) values, calculated from the data shown in Fig. 2, are presented in Table 1. The M_{RS} value of the empty sample holder is more than one order of magnitude less than the lowest value measured for ferrihydrite. Values of M_{RS} for 2-line range from 0.160 ± 0.001 A m^{-1} (1σ) (freeze-dried) to 1.34 ± 0.01 A m^{-1} (1σ)

Table 1
Susceptibility and saturation remanent magnetization data

Sample		Volume specific units (Measured)		Mass specific units (Calculated)	
		Susceptibility κ_{SI} (10^{-3})	Saturation remanent magnetization M_{RS} (A m^{-1})	Susceptibility χ (10^{-6} m^3 kg^{-1})	Saturation remanent magnetization σ_{RS} (10^{-3} A m^3 kg^{-1})
Ferrihydrite 2-line	Wet	6.460 (7)	1.34 (1)	1.700 (2)	0.35 (0)
(Nitrate)	Dry	10.08 (1)	0.451 (2)	2.65 (0)	0.119 (0)
Ferrihydrite 2-line	Wet	5.577 (6)	0.41 (1)	1.468 (2)	0.11 (0)
(Chloride)	Dry	8.200 (9)	0.160 (1)	2.158 (2)	0.042 (3)
Ferrihydrite 6-line	Wet	7.242 (8)	0.157 (3)	1.906 (2)	0.041 (1)
	Dry	10.24 (1)	0.325 (1)	2.69 (0)	0.086 (1)
Goethite	Dry	5.157 (6)	16.48 (1)[a]	1.357 (1)	64 (0)[b]
JDF	Dry	4.037 (3)	10.154 (1)	1.062 (1)	2.67 (0)
SP1	Wet	0.488 (4)	5.17 (1)	0.129 (1)	1.36 (0)
	Dry	3.07 (3)	10.57 (3)	0.81 (1)	2.178 (7)
SP2	Wet	7.721 (4)	27.652 (2)	2.032 (1)	7.28 (0)
	Dry	9.529 (4)	28.854 (2)	2.508 (1)	7.59 (0)

The mass specific susceptibility and saturation remanent magnetization values were calculated for synthetic (2- and 6-line)ferrihydrite and natural samples (JDF, SP1, SP2) from the measured volume specific data (see text for details). [a] Isothermal remanent magnetization value at 1200 mT for synthetic goethite. [b] Mass specific saturation magnetization value extrapolated from 1200 mT for synthetic goethite (see text for details). JDF—Axial Volcano, Juan de Fuca mid-ocean ridge. SP1, SP2—Spring samples from Aspo Hard Rock laboratory (HRL) in southern Sweden. Errors (1σ) are shown in brackets and correspond to the last decimal place.

(wet). Six-line ferrihydrite yields M_{RS} values of 0.157 ± 0.003 A m^{-1} (1σ) (wet) and 0.325 ± 0.001 A m^{-1} (1σ) (freeze-dried). The corresponding mass specific saturation remanent magnetization (σ_{RS}) values (Table 1) were calculated by dividing M_{RS} by density (3.96 g cm^{-3}, [37]) [35].

Hysteresis measurements for both 2-line and 6-line ferrihydrite show similar results with a linear irreversible magnetization curve at lower fields (<150 mT) and a sigmoidal-like behaviour at higher fields (>150 mT) (Fig. 3). The linearity at low fields suggests the presence of a paramagnetic component. The sigmoidal behaviour, displaying hysteresis, indicates the presence of a weakly saturating superparamagnetic component [41]. However, the magnetization curves do not exhibit hysteresis loops that are characteristic of

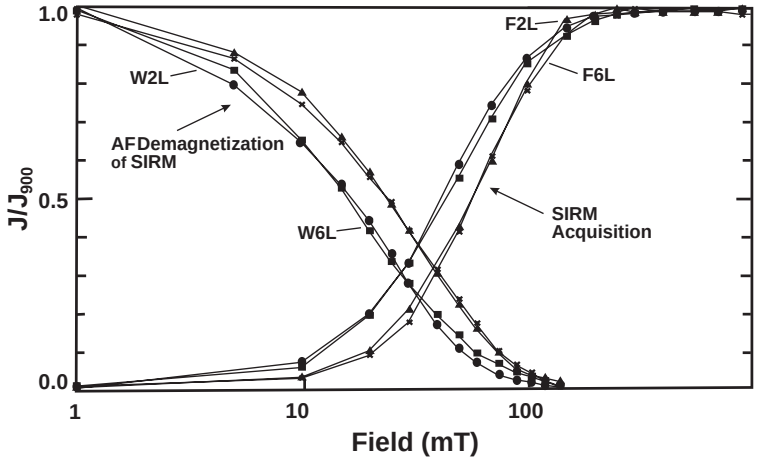

Fig. 2. Cross-over plots depicting saturation isothermal remanent magnetization (SIRM) acquisition and decay curves. Solid circles are wet 2-line ferrihydrite (W2L), solid squares are wet 6-line ferrihydrite (W6L), triangles are freeze-dried 2-line ferrihydrite (F2L) and crosses are freeze-dried 6-line ferrihydrite (F6L).

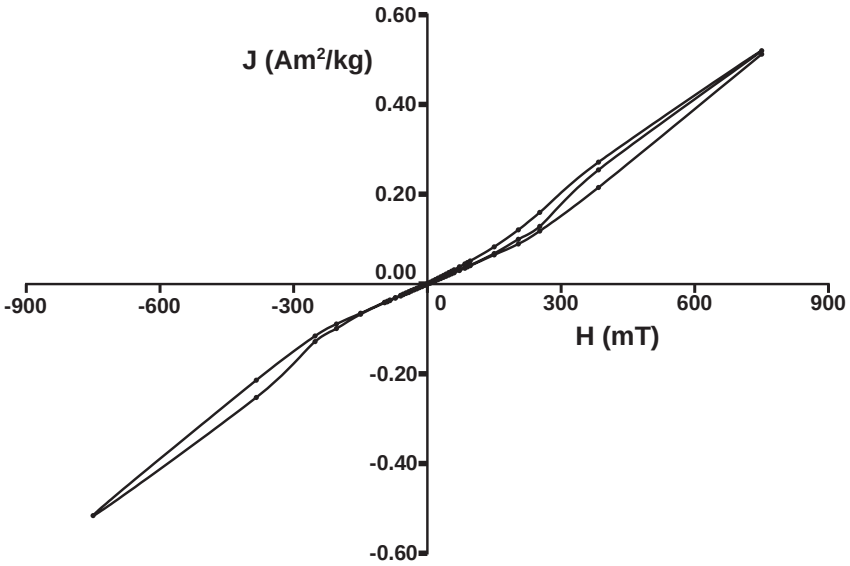

Fig. 3. Hysteresis loops for 2-line ferrihydrite at room temperature.

ferromagnetic/ferrimagnetic minerals such as magnetite or maghemite. The saturation of magnetization demonstrated in the SIRM tests is not reflected in hysteresis loops. The reason for this is not clear but may be related to behavioural differences of superparamagnetic components in the presence or absence of applied fields.

3.2. Mixtures of ferrihydrite and goethite

Cross-over plots are presented in Fig. 4a showing the remanent magnetization acquisition and the subsequent AF demagnetization curves for mixtures (M1–M5, Table 2) of ferrihydrite and goethite. The mass concentration of goethite, which increases from M1 to M5, is clearly reflected in the cross-over plots. Curve M1 (99.81% ferrihydrite) exhibits a remanent magnetization acquisition, which saturates at ~200 mT, and a systematic AF decay of σ_{RS} that are both characteristic of synthetic ferrihydrite (Fig. 2). Both acquisition and AF decay curves shift systematically with progressive increases in goethite concentration towards type curves characteristic of goethite. Curve M5 (50.00% ferrihydrite) falls dominantly within the pseudosingle domain (PSD) field for goethite with the remanent magnetization continuing to increase with increasing applied field. Fig. 3b shows absolute magnetization acquisition curves for the mixtures M1 and M4. These curves illustrate that mixture M1 saturates while mixture M4 does not saturate below 1200 mT.

3.3. Natural samples

The XRD pattern for JDF shows that this sediment is comprised entirely of poorly crystalline material (Fig. 5a). The two broad peaks at ~0.15 and 0.25–0.26 nm are characteristic of 2-line ferrihydrite [25]. Similarly, the XRD patterns derived from the HRL spring samples (Fig. 5b, c) demonstrate the absence of crystalline Fe minerals. HRL sample SP2 exhibits a pattern similar to 6-line ferrihydrite. The κ_{SI} values of freeze-dried natural sediments are 4.037 ± 0.003, 3.07 ± 0.03 and $9.529 \pm 0.004 \times 10^{-3}$ (1σ) for samples JDF, SP1 and SP2, respectively. The equivalent χ values for these sediments (Table 1) have been calculated as above based on a density of 3.96 g cm^{-3}. This calculation is subject to the assumption that the sample is comprised entirely of ferrihydrite. A similar approach was used to calculate the σ_{RS} values from M_{RS} for these sediment samples (Table 1). The M_{RS} values for JDF, SP1 and SP2 are 16.481 ± 0.008, 10.57 ± 0.03 and 28.854 ± 0.002 A m^{-1} (1σ), respectively.

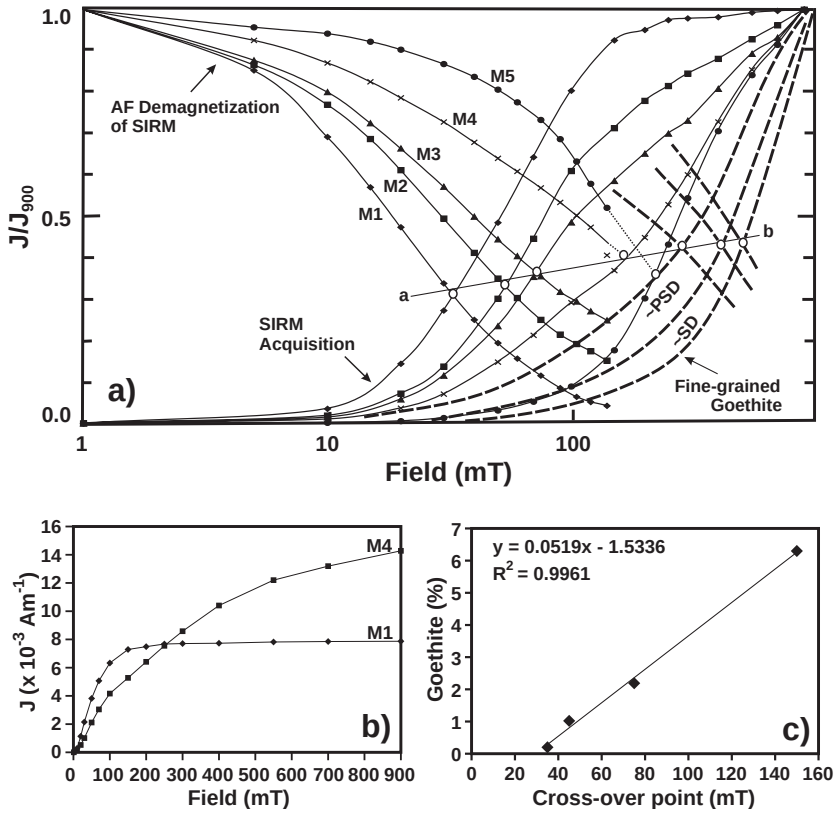

Fig. 4. Magnetic properties of mixtures (a) cross-over plots depicting SIRM acquisition and decay curves for mixtures M1 (solid diamonds), M2 (solid squares), M3 (solid triangles), M4 (crosses), M5 (solid circles); Line AB illustrates the trend of changing cross-over point (applied field) with the change in the goethite fraction, (b) absolute isothermal remanent intensity for M1 and M4, and (c) plot of the applied field vs. the percentage fraction of goethite (the linear equation was derived by least squares regression).

Cross-over plots for JDF, SP1 and SP2 are presented in Fig. 6. The acquisition and AF decay curves for JDF show a cross-over point that falls inside the ferrihydrite field with the magnetization saturating below 1200 mT (Fig. 6a). The freeze-dried SP1 and SP2 samples show acquisition and AF decay curves (Fig. 6b), with a saturation magnetization of ~200 mT, similar to synthetic ferrihydrite.

Table 2
Mixtures of ferrihydrite and goethite

Mixtures	Goethite (%)	Ferrihydrite (%)
M1	0.19	99.81
M2	1.02	98.98
M3	2.19	97.81
M4	6.30	93.70
M5	50	50

4. Discussion

4.1. Room-temperature magnetic properties of ferrihydrite

The room-temperature magnetic properties of ferrihydrite have been largely overlooked as potential tools in geophysical, geochemical and environmental research as a result of several factors including the initial reports of Néel temperatures below 298 K [40,41] and the disagreement over the nature and extent of crystallographic ordering [1–3,5]. However, recent work [5,44] has determined Néel temperatures of 350 and 330 ± 20 K for nanocrystalline ferrihydrite, which suggests that ferrihydrite can exhibit magnetic ordering at room temperature. Furthermore, Zergenyi et al. [41] have identified a parasitic ferromagnetic component in synthetic 6-line ferrihydrite.

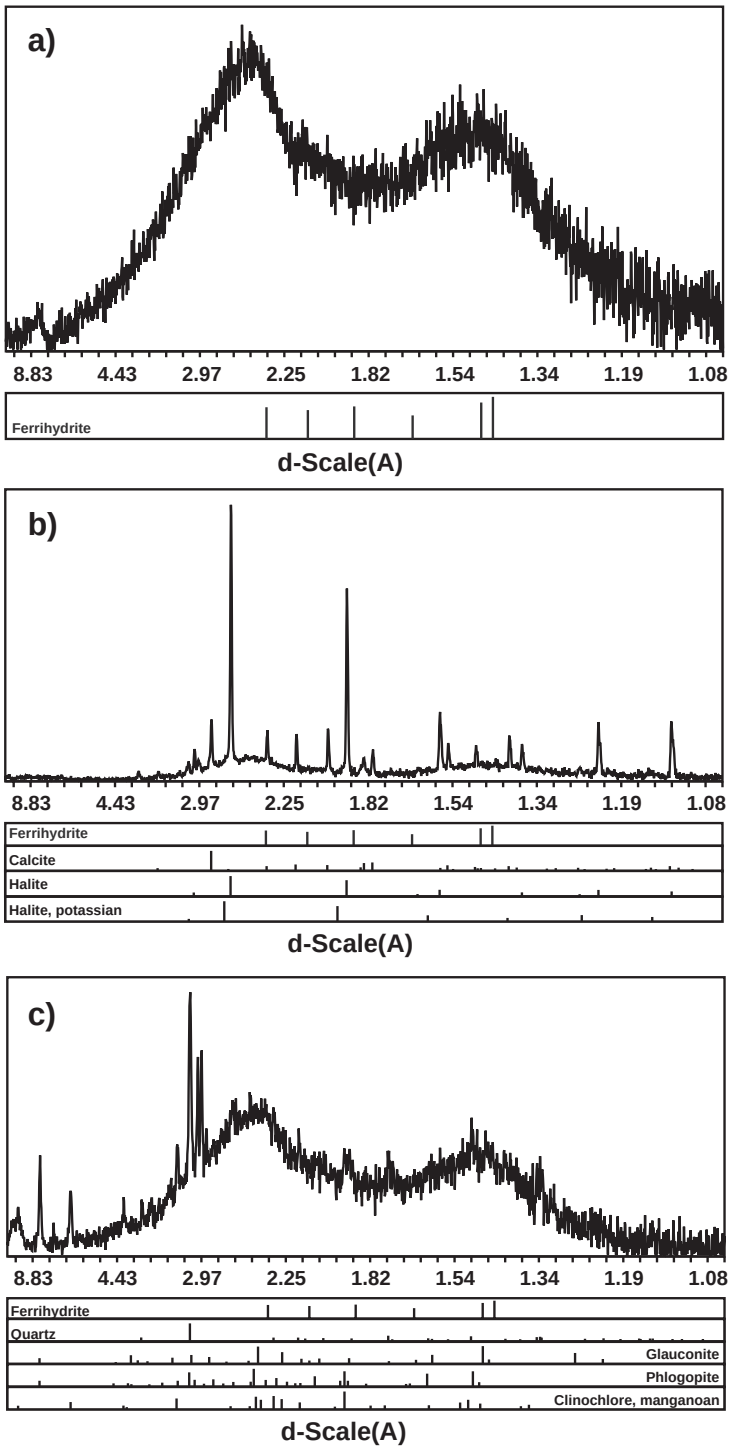

Fig. 5. Powder XRD patterns for natural samples (a) Axial volcano, Juan de Fuca ridge (JDF), (b) Hard Rock Laboratory (SP1), and (c) Hard Rock Laboratory (SP2).

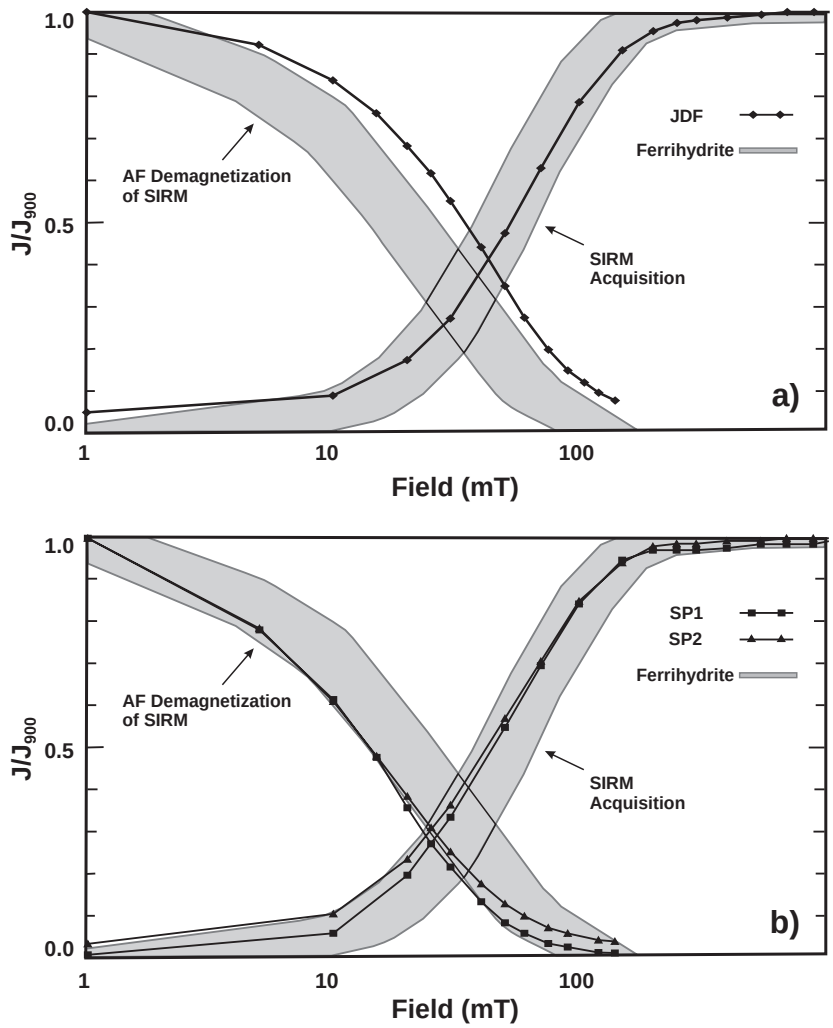

Fig. 6. Cross-over plots depicting SIRM acquisition and decay curves for natural samples, (a) Axial volcano, Juan de Fuca ridge (JDF), and (b) Hard Rock Laboratory (SP1) and Hard Rock Laboratory (SP2).

This work presents the first documentation of a room-temperature magnetic susceptibility for 2-line ferrihydrite. In keeping with the units presented in Peters and Dekkers [35], the preferred χ value is 2.652 ± 0.003 A m^2 kg^{-1} (1σ) for 2-line ferrihydrite. In addition, the χ value of 2.694 ± 0.003 A m^2 kg^{-1} (1σ) obtained for 6-line ferrihydrite is similar to the value given by Zergenyi et al. [41]. The small difference may be attributed to differences in the synthesis techniques used between studies. These values, along with a comparison to average χ values for other Fe minerals [35], are given in Table 3. The calculated χ of $1.357 \pm 0.002 \times 10^{-6}$ m^3 kg^{-1} (1σ) for the synthetic goethite measured in this work is in good agreement with the average value of 1.17×10^{-6} m^3 kg^{-1} (1σ) given by Peters and Dekkers [35]. This gives confidence in the validity of the calculation made to convert κ_{SI} to χ for ferrihydrite. Although the χ values for ferrihydrite are based on a poorly-constrained density value, it is not expected that this value is in error by more than a few percent, which is well within the variation in χ that results from the range of κ_{SI} observed for synthetic samples. Furthermore, the conversion

Table 3
Comparative magnetic properties of iron minerals

Mineral	Susceptibility χ (10^{-6} m^3 kg^{-1})	Saturation remanent magnetization σ_{RS} (A m^2 kg^{-1})
Ferrihydrite (2-line)[a]	2.652 (3)	1.19×10^{-4} (0)
Ferrihydrite (6-line)[a]	2.694 (3)	0.86×10^{-4} (1)
Ferrihydrite (6-line)[b]	1.00 (1)	NA
Goethite—this study[a]	1.357 (2)	0.064 (0)
Goethite—literature	1.17	0.05
Magnetite	674	5.3
Titanomagnetite	422	5.2
Maghemite	632	6.8
Hematite	0.97	0.18
Greigite	108	5.4
Pyrrhotite	32.1	5.0

[a] Mass specific values for synthetic (2- and 6-line) ferrihydrite and goethite. [b] Mass specific values for 6-line ferrihydrite from Zergenyi et al. [41]. All other values are from Peters and Dekkers [35]. Errors (1σ) are shown in brackets and correspond to the last decimal place.

from κ_{SI} to χ may be easily re-calculated to remain consistent with better constrained density data. In comparison to other Fe oxyhydroxides, ferrihydrite has a susceptibility that is similar to the values of both goethite and hematite but is two orders of magnitude lower than the values of magnetite and maghemite. This suggests that χ would be useful for identifying trace amounts of magnetite in dominantly ferrihydrite systems. Such a situation would be common near redox boundaries in lacustrine systems where rapid fluctuations in redox conditions preclude the formation of more stable oxidized minerals (i.e. hematite and goethite) [12]. Under these conditions microbial Fe reduction would likely result in the rapid formation of small amounts of persistent magnetite [15,16]. Thus, measurements of χ may have useful applications in studies of redox transformations in natural systems.

In addition to susceptibility, the SIRM behaviour has been investigated using cross-over plots [47]. Significantly, ferrihydrite has been found to saturate at fields of ~200 mT. Furthermore, the SIRM acquisition and decay curves plot within the type curves for single domain and pseudosingle domain magnetite (Fig. 7). Based on this, it is reasonable to suspect that the observed magnetic behaviour for these synthetic samples is caused by the presence of low concentrations of magnetite contamination.

To test this hypothesis, low-temperature susceptibility profiles have been measured for both synthetic 2- and 6-line ferrihydrite. A plot of these profiles is presented in Fig. 8a. If there was magnetite in the samples, it would be expected that these profiles would exhibit the characteristic Verwey transition at 120 K [48]. However, the low-temperature susceptibility profiles show no deviation from the smooth trend that is characteristic of ferrihydrite [41,44]. In addition, another potential contaminant that may contribute to the observed susceptibility is maghe-

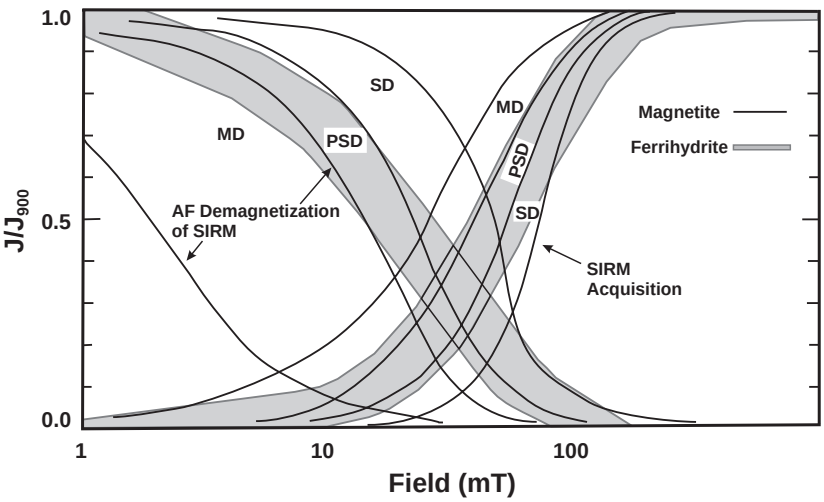

Fig. 7. Cross-over plots depicting type curves of SIRM acquisition and decay for magnetite [45] and the field derived for synthetic ferrihydrite. SD=single-domain, PSD=pseudo-single domain, MD=multi-domain.

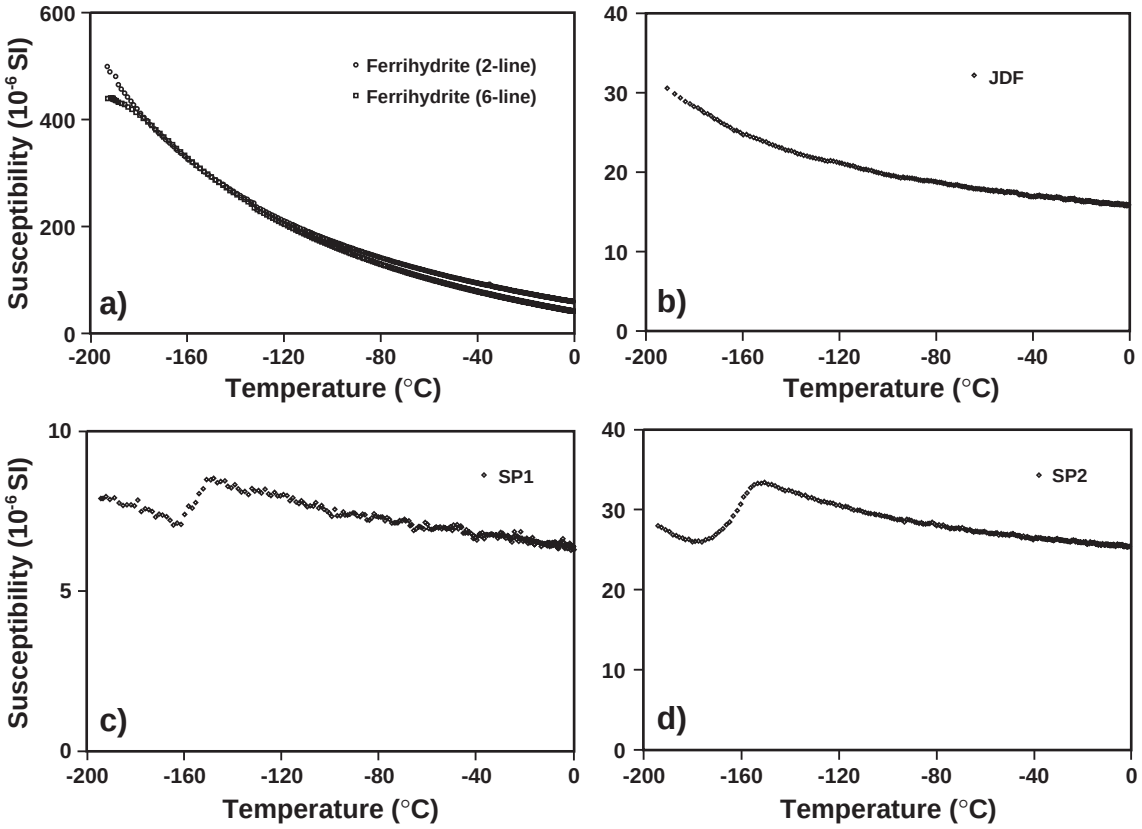

Fig. 8. Low-temperature magnetic susceptibility curves (a) synthetic 2-line (open circles) and 6-line (open squares) ferrihydrite, (b) Axial volcano, Juan de Fuca ridge (JDF), (c) Hard Rock Laboratory (SP1), and (d) Hard Rock Laboratory (SP2).

mite. However, maghemite lacks any distinct low temperature transition. There was no evidence for maghemite contamination in either hysteresis loops and/or electron microscopy. Furthermore, based on the synthesis protocols used in this study (i.e. formation using Fe(III) salt solutions under oxidizing conditions) there is no a priori reason to expect magnetite in the synthetic ferrihydrite samples. Thus, the observed cross-over patterns and the saturation behaviour can be attributed to ferrihydrite. In contrast to the more crystalline Fe (III) oxyhydroxides, goethite and hematite, which saturate under exceedingly high magnetic fields (goethite — ~20,000 mT, hematite — ~25,000 mT, [49,50]), synthetic ferrihydrite saturates at ~200 mT. As a result, the mass specific value of the saturation magnetization can be easily obtained.

This work presents the first documentation of saturation magnetization values for ferrihydrite. Again to remain consistent with the work of Peters and Dekkers [35], the recommended values for saturation remanent magnetization are 1.19 ± 0.0001 and $0.86 \pm 0.001 \times 10^{-4}$ A m^2 kg^{-1}(1σ) for 2- and 6-line ferrihydrite, respectively. These values, along with the literature values [35], are presented in Table 3. As goethite saturates at very high field strengths of ~20,000 mT [49], it is not possible to measure the σ_{RS} using the Sapphire Instruments SI-6 pulse magnetizer with a maximum field of 2000 mT. The measured remanent magnetization value obtained at 1200 mT for the synthetic goethite was used to calculate a theoretical σ_{RS} value by linear extrapolation to 20,000 mT. This value, 0.06 A m^2 kg^{-1}, is in good agreement with the average σ_{RS} value of 0.052 A m^2 kg^{-1} [35]. This gives confidence in both the measurement protocols and calculation procedures used to obtain values of σ_{RS} for ferrihydrite.

The remanent acquisition and decay behaviour suggest that ferrihydrite has a weak ferromagnetic component at room temperature. This component could arise from uncompensated surface spins that may result in nanoparticle interactions [44]. However, further detailed examination of ferrihydrite, both 2- and 6-line, is required to further constrain the origin of the ferromagnetic component. Importantly, the ferromagnetic behaviour at room temperature suggests that ferrihydrite is capable of carrying remanent magnetization in environmental or geological samples. In addition, the ability of ferrihydrite to retain a remanent magnetization is consistent with a structural model that involves a degree of internal ordering.

4.2. Quantifying ferrihydrite in mixtures with goethite

Mineral magnetic properties are often used to quantify the relative proportions of different minerals in natural samples [33–35]. A common problem in environmental studies of soils and aquatic sediments is the discrimination between amorphous or poorly crystalline Fe and Mn oxyhydroxides (e.g., ferrihydrite, MnO_2), which are highly reactive [12], and the more crystalline counterparts (e.g. goethite, hematite, pyrolusite) which are less reactive. As the former lack well ordered structures, they are not amenable to conventional XRD techniques. Thus, operationally defined chemical extractions (e.g., [32,51]) are often used, however, these techniques are fraught with complications that arise from matrix variability [16,24]. Based on the observed magnetic behaviour of ferrihydrite, notably its magnetization saturation in relatively weak fields compared to goethite and hematite, cross-over plots [47] provide a promising approach for quantifying mixtures of these minerals.

Fig. 4a illustrates the systematic change in the cross-over points with increasing goethite concentration from 0.2% to 50%. For this mixture it is possible to quantify the percentage of goethite based on a linear variation in the value of the applied field at the cross-over point. This relationship is shown in Fig. 4c. In systems where goethite is present, it will overwhelm the XRD pattern and render ferrihydrite or other poorly crystalline phases undetectable. In these systems it may be pertinent to use magnetization characteristics to quantify the presence of small amounts of goethite in mixtures with ferrihydrite. However, Fig. 4b illustrates that for mixtures of greater than ~5% goethite, the goethite remanent intensity is more than twice that of ferrihydrite and therefore dominates the cross-over plot characteristics. The relative σ_{RS} intensities of ferrihydrite and goethite may also explain why the remanence characteristics have remained elusive to date.

4.3. Application to natural samples

In order to evaluate the utility of using room-temperature magnetic properties to characterize ferrihydrite in natural samples, the magnetic properties of sediments from the HRL and JDF have been characterized. The XRD patterns for these samples show the absence of other Fe minerals (Fig. 5). The pattern derived for JDF is characteristic of 2-line ferrihydrite. The pattern derived for SP2 is also similar to ferrihydrite but, in addition, shows a peak characteristic of quartz at ~0.33 nm. In SP1 the presence of small amounts of calcite and halite preclude the identification of the ferrihydrite pattern. Both calcite and halite are diamagnetic and therefore may weakly influence measurements of χ.

The values of χ for all three sediment samples indicate that they are comprised dominantly of low susceptibility Fe minerals such as goethite, hematite, or ferrihydrite. However, the saturating field is <1200 mT which is characteristic of ferrihydrite and negates the presence of goethite or hematite. Although it is not possible to isolate ferrihydrite as the only mineral in the samples, the low values of χ are inconsistent with the presence of even trace amounts of pyrrhotite and magnetite.

To further test for the presence of trace amounts of magnetite in these sediments low-temperature susceptibility profiles have been obtained (Fig. 8b, c, d). The absence of the Verwey transition in the JDF sample (Fig. 8b) gives confidence in the conclusion that negligible magnetite is present and that this sample is comprised overwhelmingly of ferrihydrite. In contrast, the presence of the Verwey transition in both samples SP1 and SP2 suggests trace amounts of magnetite. However, both the absence of magnetite peaks in the XRD pattern and the low χ values suggest that both samples SP1 and SP2 are comprised dominantly of ferrihydrite.

5. Conclusions

The magnetic susceptibilities of both 2- and 6-line ferrihydrite are similar to goethite and hematite, but are two orders of magnitude lower than maghemite, pyrrhotite and magnetite. Both varieties of ferrihydrite have been found to saturate in fields of less than 1200 mT at room temperature. This implies that the coercivity of ferrihydrite is much lower than goethite and hematite, which require saturation fields in excess of ~20,000 mT. Based on an analogy to low coercivity minerals (i.e. magnetite and pyrrhotite), the magnetic properties of ferrihydrite suggests a weak ferromagnetic behaviour at room temperature. Importantly, this means that ferrihydrite has the potential to carry a natural magnetic remanence (NRM) and the study of it may provide unique insights into the early diagenesis of Fe-rich sediments. Additionally, χ and σ_{RS} are useful parameters for discriminating ferrihydrite in natural samples. The measured magnetic properties suggest that due to its weak remanence, often attributed to other Fe-phases, ferrihydrite is probably overlooked in natural systems.

Acknowledgements

The authors are indebted to Dr. Chris Kennedy, University of Götenberg, Sweden, for providing natural samples of ferrihydrite and Fred Pearson, Brockhouse Institute for Materials Research, McMaster University, for the contributed TEM images. Ezra Kulcyzki is acknowledged for help in preparation of the synthetic samples. The authors also thank Dr. Mike Jackson and an anonymous reviewer for their helpful suggestions. Funding was provided by NSERC, CRC, PREA and Discovery grants to DAF, and Discovery grants to MTC and DTAS.

References

[1] A. Manceau, V.A. Drits, Local-structure of ferrihydrite and feroxyhite by EXAFS spectroscopy, Clay Miner. 28 (1993) 165–184.

[2] D.E. Janney, J. Cowley, M.P.R. Buseck, Structure of synthetic 2-line ferrihydrite by electron nanodiffraction, Am. Mineral. 85 (2000) 1180–1187.

[3] D.E. Janney, J. Cowley, M.P.R. Buseck, Structure of synthetic 6-line ferrihydrite by electron nanodiffraction, Am. Mineral. 86 (2001) 327–335.

[4] D.G. Rancourt, D. Fortin, T. Picheler, P.-J. Thibault, G. Lamarche, R.V. Morris, P.H.J. Mercier, Mineralogy of a natural As-rich ferric oxide co-precipitate formed by mixing of hydrothermal fluid and seawater: implications regarding surface complexation and color banding in ferrihydrite deposits, Am. Mineral. 86 (2001) 834–851.

[5] E. Jansen, A. Kyek, W. Shafer, U. Schwertmann, The structure of six-line ferrihydrite, Appl. Phys., A 74 (2002) S1004–S1006.

[6] U. Schwertmann, L. Carlson, E. Murad, Properties of iron-oxides in 2 Finnish lakes in relation to the environment of their formation, Clays Clay Miner. 35 (1987) 297–304.

[7] D. Fortin, G.G. Leppard, A. Tessier, Characteristics of lacustrine diagenetic iron oxyhydroxides, Geochim. Cosmochim. Acta 57 (1993) 4391–4404.

[8] Y. Shaked, Y. Erel, A. Sukenik, The biogeochemical cycle of iron and associated elements in Lake Kinneret, Geochim. Cosmochim. Acta 68 (2004) 1439–1451.

[9] A.J. Brearley, Nature and origin of matrix in the unique type-3 chondrite, Kakangari, Geochim. Cosmochim. Acta 53 (1989) 2395–2411.

[10] J.L. Bishop, C.M. Pieters, R.G. Burns, Reflectance and Mossbauer-spectroscopy of ferrihydrite–montmorillonite assemblages as Mars soil analog materials, Geochim. Cosmochim. Acta 57 (1993) 4583–4595.

[11] R.V. Morris, D.C. Golden, J.F. Bell III, H.V. Lauer Jr., J.B. Adams, Pigmenting agents in Martian soils—inferences from spectral, Mossbauer, and magnetic properties of nanophase and other iron oxides in Hawaiian Palagonitic soil PN-9, Geochim. Cosmochim. Acta 57 (1993) 4597–4609.

[12] W. Stumm, B. Sulzberger, The cycling of iron in natural environments—considerations based on laboratory studies of heterogeneous redox processes, Geochim. Cosmochim. Acta 56 (1992) 3233–3257.

[13] S.L.S. Stipp, M. Hansen, R. Kristensen, M.F. Hochella Jr., L. Bennedsen, K. Dideriksen, T. Balic-Zunic, D. Leonard, H.-J. Mathieu, Behaviour of Fe-oxides relevant to contaminant uptake in the environment, Chem. Geol. 190 (2002) 321–337.

[14] B. Müller, L. Granina, T. Schaller, A. Ulrich, B. Wehrli, P, As, Sb, Mb and other elements in sedimentary Fe/Mn layers of Lake Baikal, Environ. Sci. Technol. 36 (2002) 411–420.

[15] D.R. Lovely, J.F. Stolz, G.L. Nord Jr., E.J.P. Phillips, Anaerobic production of magnetite by a dissimilatory iron-reducing microorganism, Nature 330 (1987) 252–254.

[16] J.M. Zachara, R.K. Kukkadapu, J.K. Frederickson, Y.A. Gorby, S.C. Smith, Biomineralization of poorly crystalline Fe (III) oxides by dissimilatory metal reducing bacteria (DMRB), Geomicrobiol. J. 19 (2002) 179–207.

[17] C.B. Kennedy, S.D. Scott, F.G. Ferris, Characterization of bacteriogenic iron oxide deposits from Axial Volcano, Juan de Fuca Ridge, northeast Pacific Ocean, Geomicrobiol. J. 20 (2003) 199–214.

[18] D. Soblev, E.E. Roden, Suboxic deposition of ferric iron by bacteria in opposing gradients of Fe (II) and oxygen at

circumneutral pH, Appl. Environ. Microbiol. 67 (2001) 1328–1334.
[19] F.V. Chukhrov, B.B. Zvyagin, A.I. Gorshkov, L.P. Yermilova, V.V. Balashova, Ferrihydrite, Int. Geol. Rev 16 (1974) 1131–1143.
[20] F.G. Ferris, K. Tazaki, W.S. Fyfe, Iron-oxides in acid-mine drainage environments and their association with bacteria, Chem. Geol. 74 (1989) 321–330.
[21] C.B. Kennedy, R.E. Martinez, S.D. Scott, F.G. Ferris, Surface chemistry and reactivity of bacteriogenic iron oxides from Axial Volcano, Juan de Fuca Ridge, north-east Pacific Ocean, Geobiology 1 (2003) 59–69.
[22] M. Vargas, K. Kashefi, E.L. Blunt-Harris, D.R. Lovley, Microbiological evidence for Fe (III) reduction on early Earth, Nature 395 (1998) 65–67.
[23] C.W. Childs, Ferrihydrite—a review of structure, properties and occurrence in relation to soils, Zeitschrift Fur Pflanzenernahrung Und Bodenkunde 155 (1992) 441–448.
[24] J.L. Jambor, J.E. Dutrizac, Occurrence and constitution of natural and synthetic ferrihydrite, a widespread iron oxyhydroxide, Chem. Rev. 98 (1998) 2549–2585.
[25] R.M. Cornell, U. Schwertmann, The Iron Oxides: Structure, Properties, Reactions, Occurrence, and Uses, Wiley-VCH, Weinheim, 1996, 573 pp.
[26] U. Schwertmann, R.M. Cornell, Iron Oxides in the Laboratory, VCH, New York, 1991, 137 pp.
[27] J.M. Combes, A. Manceau, G. Calas, J.Y. Bottero, Formation of ferric oxides from aqueous solution—a polyhedral approach by X-ray absorption-spectroscopy: 1. Hydrolysis and formation of ferric gels, Geochim. Cosmochim. Acta 53 (1989) 583–594.
[28] J.M. Combes, A. Manceau, G. Calas, Formation of ferric oxides from aqueous-solutions—a polyhedral approach by X-ray absorption-spectroscopy: 2. Hematite formation from ferric gels, Geochim. Cosmochim. Acta 54 (1990) 1083–1091.
[29] A. Manceau, J.M. Combes, G. Calas, New data and a revised structural model for ferrihydrite—comment, Clays Clay Miner. 38 (1990) 331–334.
[30] J.M. Zhao, F.E. Huggins, Z. Feng, F.L. Lu, N. Shah, G.P. Huffman, Structure of a nanophase iron-oxide catalyst, J. Catal. 143 (1993) 499–509.
[31] J.M. Zhao, F.E. Huggins, Z. Feng, G.P. Huffman, Ferrihydrite—surface structure and its effects on phase-transformation, Clays Clay Miner. 42 (1994) 737–746.
[32] U. Schwertmann, Use of oxalate for iron extraction from soils, Can. J. Soil Sci. 53 (1973) 244–246.
[33] K.L. Verosub, A.P. Roberts, Environmental magnetism: past, present and future, J. Geophys. Res. 100 (B2) (1995) 2175–2192.
[34] D.J. Dunlop, Magnetism in rocks, J. Geophys. Res. 100 (1995) 2161–2174.
[35] C. Peters, M.J. Dekkers, Selected room temperature magnetic properties as a function of mineralogy, concentration and grain size, Phys. Chem. Earth 28 (2003) 659–667.
[36] T. Frederichs, T. von Dobeneck, U. Bleil, M.J. Dekkers, Towards the identification of siderite, rhodochrosite and vivianite in sediments by the low temperature magnetic properties, Phys. Chem. Earth 28 (2003) 669–679.
[37] K.M. Towe, W.F. Bradley, Mineral constitution of colloidal "hydrous ferric oxides", J. Colloid Interface Sci. 24 (1967) 384–392.
[38] E. Murad, U. Schwertmann, The Mössbauer spectrum of ferrihydrite and its relations to those of other iron oxides, Am. Mineral. 65 (1980) 1044–1079.
[39] E. Murad, The Mössbauer spectrum of "well"-crystallized ferrihydrite, J. Magn. Magn. Mater. 74 (1988) 153–157.
[40] Q.A. Pankhurst, R.J. Pollard, Structural and magnetic properties of ferrihydrite, Clays Clay Miner. 40 (1992) 268–272.
[41] R.S. Zergenyi, A.M. Hirt, J.P. Zimmermann, J.P. Dobson, W. Lowrie, Low-temperature magnetic behaviour of ferrihydrite, J. Geophys. Res. 105 (2000) 8297–8303.
[42] M.C. Grantham, P.M. Dove, Investigation of bacterial–mineral interactions using fluid tapping mode (TM) atomic force microscopy, Geochim. Cosmochim. Acta 60 (1996) 2473–2480.
[43] J.F. Banfield, S.A. Welch, H. Zhang, T.T. Ebert, R.L. Penn, Aggregation-based crystal growth and microstructure development in natural iron oxyhydroxide biomineralization products, Science 289 (2000) 751–754.
[44] M.S. Seehra, V.S. Babu, A. Manivannan, J.W. Lynn, Neutron scattering and magnetic studies of ferrihydrite nanoparticles, Phys. Rev., B 61 (2000) 3513–3518.
[45] K. Pederson, Microbial life in deep granitic rocks, FEMS Microbiol. Rev. 20 (1997) 399–414.
[46] R.M. Cornell, U. Schwertmann, The Iron Oxides: Structure, Properties, Reactions, Occurrence, and Uses, Wiley-VCH, Weinheim, 2003, 664 pp.
[47] D.T.A. Symons, M.T. Cioppa, Crossover plots: a useful method for plotting SIRM data in paleomagnetism, Geophys. Res. Lett. 27 (2000) 1779–1782.
[48] E.J. Verwey, Electronic conduction of magnetite (Fe_3O_4) and its transition points at low temperatures, Nature 144 (1939) 327–328.
[49] M.J. Dekkers, Magnetic properties of natural goethite: I. Grain-size dependence of some low- and high-field related rockmagnetic parameters measured at room temperatures, Geophys. J. Int. 97 (1989) 323–340.
[50] D.J. Dunlop, Ö. Özdemir, Rock Magnetism: Fundamentals and Frontiers, Cambridge University Press, Cambridge, 1997, 573 pp.
[51] D.R. Lovely, E.J.P. Phillips, Rapid assay for microbially reducible ferric iron in aquatic sediments, Appl. Environ. Microbiol. 53 (1987) 1536–1540.